Available online on 15.03.2019 at http://jddtonline.info

Journal of Drug Delivery and Therapeutics

Open Access to Pharmaceutical and Medical Research

Open Access Research Article

Comparative Molecular Field Analysis on 4(3H) Quinazolinone derivatives for the Development of Potential Antimicrobial Agents

Sumit Bhattacharya [a], Vaibhav Rajoriya [b], Pradip Jana [b] and Varsha Kashaw [a*]

[a] SVN Institute of Pharmaceutical Sciences, Swami Vivekanand University, Sagar, Madhya Pradesh, India

[b] Department of Pharmaceutical Sciences, Dr. Harisingh Gour University (A Central University), Sagar, (M.P.) 470003, India

ABSTRACT

Objective: Objective of present paper was to perform comparative Molecular Field Analysis on 4(3H) Quinazolinone derivatives for the Development of Potential Antimicrobial Agents.

Method: 4(3H)-quinazolinone is one of the most frequently studied heterocyclic moiety possessing wide range of biological activities. Three dimensional quantitative structure activity analysis (3D QSAR) has been carried out on some already reported 4(3H)-quinazolinone derivatives to explore the structural requirements for antifungal and antibacterial activities. QSAR models were generated with comparative molecular field analysis (CoMFA) using partial least square (PLS) method. CoMFA descriptors were calculated on aligned structures to understand the steric and electrostatic field contribution on the biological activity.

Result and Discussion: The generated CoMFA models for antifungal activity showed a cross-validation coefficient (q^2) of 0.578, non-cross validation coefficient (r^2) of 0.923 and standard error of 0.0177. The predictive ability of the model was validated using external validation with predictive factor (r^2_{pred}) of 0.94 for antifungal activity. The significant statistical parameters indicated the reliability and good predictive power of the developed model. The 3D contour maps generated from CoMFA models were analyzed for key structural requirements for improved activity.

Conclusion: This study will help to further optimize quinazoline-4(3H)-one derivatives for antimicrobial activities.

Keywords: 4(3H)-quinazolinones; 3D QSAR; Comparative molecular field analysis (CoMFA); antifungal activity; antibacterial activity.

Article Info: Received 12 Jan 2019; Review Completed 04 March 2019; Accepted 10 March 2019; Available online 15 March 2019

Cite this article as:

BhattacharyaS , Rajoriya V, Jana P, Kashaw V Comparative Molecular Field Analysis on 4(3H) Quinazolinone derivatives for the Development of Potential Antimicrobial Agents, Journal of Drug Delivery and Therapeutics. 2019; 9(2):603-611
http://dx.doi.org/10.22270/jddt.v9i2.2706

***Address for Correspondence:**

Varsha Kashaw, SVN Institute of Pharmaceutical Sciences, Swami Vivekanand University, Sagar, Madhya Pradesh, India

INTRODUCTION

One of the most frequently encountered heterocycles in medicinal chemistry is 4(3H)-quinazolinone with wide applications including anticonvulsant, sedative, tranquilizer, analgesic, antimicrobial, anesthetic, anticancer, antihypertensive, anti-inflammatory, diuretic and muscle relaxant properties. Over the years various substitution have been made at position 2and 3 to get potent antimicrobial agents. In our earlier work we synthesized a hybrid series of 3-[5-substituted phenyl-1,3,4-thiadiazole-2-yl]-2-styryl quinazoline-4(3H)-one with potent antimicrobial activity[1].

Quantitative structure-activity relationship (QSAR) methodology is an essential tool to predict the relationship between the structure of molecules and their biological activities which is essential for the drug design and discovery. The variation in biological activities with in a series can be explained with the changes in the molecular features of compounds. The developed model through QSAR studies can also be used to predict the activities of novel molecules prior to their synthesis. It can be used to understand the structural requirements for potent biological activity or to modify the existent biological activity of a particular molecule.Thus QSAR study is a very useful tool in modern drug discovery process to get better insight into structure activity relationships. In 3D QSAR methods comparativemolecular field analyses (CoMFA) can be appliedto gain insights into how steric, electrostatic interactions influence activities[2].

In present study we have performed 3D-QSAR based comparative molecular field analysis (CoMFA) to understand

structural patterns requirements on the compound for potent the development of antimicrobial agents.

EXPERIMENTAL

Dataset

A set of 42 quinazoline-4(3H)-one derivatives and their corresponding antifungal activity (MIC in µg/ml) data in *Aspergillus nigers* (MTCC-1344) and antibacterial activity (MIC in µg/ml) data in *Bacillus subtilis* (MTCC-619) reported by Jatav *et al*., were selected[1] and used for the development of 3D QSAR CoMFA models. The dataset was randomly divided into the training set of 34 compounds (80%) to generate the 3D QSAR model, and the test set of 8 compounds (20%) to verify the predictive ability of the model. The biological activities of the compounds were represented as pMIC (-logMIC) which has been used as dependent variables. To get a good model the selection of training set and the test set was carried out in such a way that both the sets contain structurally diverse compounds and activities of all range[3]. All the structures in the dataset were sketched in ChemDraw Ultra 8.0 software.

Table 1: Chemical structures quinazoline-4(3H)-one derivatives and their antifungal and antibacterial activities.

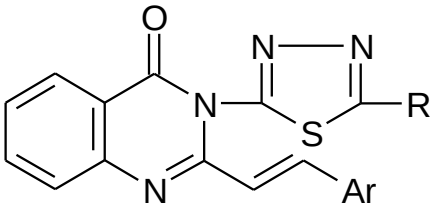

Sl.No.	Compound codes	Ar	R	Antifungal activity MIC in µg/ml	Antibacterial activity MIC in µg/ml
				A. nigers (MTCC-1344)	B. subtilis (MTCC-619)
1	4a	-C_6H_5	-C_6H_5	16.86	8.42
2	4b	-C_6H_5	p-$OCH_3C_6H_4$	17.92	7.08
3	4c	-C_6H_5	p-$CH_3C_6H_4$	14.16	6.46
4	4d	-C_6H_5	p-ClC_6H_4	15.18	7.89
5	4e	-C_6H_5	m-ClC_6H_4	15.72	7.45
6	4f	-C_6H_5	-CH=CHC_6H_4	14.62	9.92
7	4g	p-$OCH_3C_6H_4$	-C_6H_5	15.05	10.31
8	4h	p-$OCH_3C_6H_4$	p-$OCH_3C_6H_4$	17.16	6.22
9	4i	p-$OCH_3C_6H_4$	p-$CH_3C_6H_4$	17.02	5.46
10	4j	p-$OCH_3C_6H_4$	p-ClC_6H_4	16.45	6.91
11	4k	p-$OCH_3C_6H_4$	m-ClC_6H_4	13.86	6.72
12	4l	p-$OCH_3C_6H_4$	-CH=CHC_6H_4	14.08	10.49
13	4m	p-$CH_3C_6H_4$	-C_6H_5	15.87	7.99
14	4n	p-$CH_3C_6H_4$	p-$OCH_3C_6H_4$	16.63	5.12
15	4o	p-$CH_3C_6H_4$	p-$CH_3C_6H_4$	14.12	10.22
16	4p	p-$CH_3C_6H_4$	p-ClC_6H_4	14.02	9.11
17	4q	p-$CH_3C_6H_4$	m-ClC_6H_4	13.70	8.21
18	4r	p-$CH_3C_6H_4$	-CH=CHC_6H_4	16.62	7.94
19	VJ19	p-ClC_6H_4	-C_6H_5	11.32	8.32
20	VJ20	p-ClC_6H_4	p-$OCH_3C_6H_4$	12.43	4.65
21	VJ21	p-ClC_6H_4	p-$CH_3C_6H_4$	12.47	5.46
22	VJ22	p-ClC_6H_4	p-ClC_6H_4	11.88	6.46
23	VJ23	p-ClC_6H_4	m-ClC_6H_4	12.48	7.64
24	VJ24	p-ClC_6H_4	-CH=CHC_6H_4	11.76	7.63
25	VJ25	m-ClC_6H_4	-C_6H_5	12.42	6.43
26	VJ26	m-ClC_6H_4	p-$OCH_3C_6H_4$	12.68	7.48
27	VJ27	m-ClC_6H_4	p-$CH_3C_6H_4$	13.34	8.21
28	VJ28	m-ClC_6H_4	p-ClC_6H_4	12.42	7.66
29	VJ29	m-ClC_6H_4	m-ClC_6H_4	11.76	7.68
30	VJ30	m-ClC_6H_4	-CH=CHC_6H_4	12.32	10.30

31	VJ31		-C_6H_5	11.90	7.40
32	VJ32		p-$OCH_3C_6H_4$	12.24	8.32
33	VJ33		p-$CH_3C_6H_4$	12.42	9.42
34	VJ34		p-ClC_6H_4	11.48	8.47
35	VJ35		m-ClC_6H_4	10.54	7.08
36	VJ36		-$CH=CHC_6H_4$	10.94	10.75
37	VJ37	-$CH=CHC_6H_4$	-C_6H_5	13.43	7.48
38	VJ38	-$CH=CHC_6H_4$	p-$OCH_3C_6H_4$	12.48	6.40
39	VJ39	-$CH=CHC_6H_4$	p-$CH_3C_6H_4$	14.90	7.16
40	VJ40	-$CH=CHC_6H_4$	p-ClC_6H_4	15.26	9.21
41	VJ41	-$CH=CHC_6H_4$	m-ClC_6H_4	15.67	8.47
42	VJ42	-$CH=CHC_6H_4$	-$CH=CHC_6H_4$	14.82	7.44

Energy minimization of compounds

To get best conformers of each molecule the Sybyl X-2.1.1 software package was used for energy minimization. The energy minimizations were done using Tripos force field and the Powell gradient algorithm with a convergence criterion of 0.05 kcal/(mol*Å) and maximum iteration count of 1000. The partial atomic charges were calculated using Gasteiger-Huckel method[3].

Molecular Alignment rules for CoMFA modeling

Molecular alignment is one of the most essential steps for the generation of the best CoMFA models. There are various approaches suggested for molecular alignment in the literature. Some of them are:

Align Database alignment (Maximum Common Structure based alignment): This alignment is done based on maximum common structure of molecules using the most active molecule in the dataset as template.

Distill Rigid Alignment: Molecules are aligned according to their electrostatic and steric field on the template molecule.

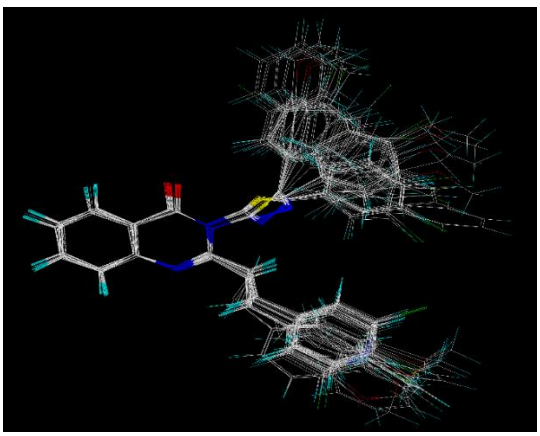

Figure 1: Distill rigid molecular alignment of molecules in the dataset.

Multifit: A number of attributes like electrostatic and steric fields, particular atom or groups, etc. can be used for alignment of the molecules to the template molecule by flexible fitting.

In the present study Align database and Distill Rigid alignment type were used. The template molecule used was the most potent molecule in the dataset.

CoMFA studies

In the CoMFA method steric and electrostatic fields were calculated using Lennard-Jones and Coulombic potentials respectively. A 3D cubic lattice with a grid spacing of 2.0 Å, was generated automatically to surround the aligned molecules in all directions. These grid points were generated using the Tripos force field, a sp^3 carbon atom probe with a Van der Waals radius of 1.52 Å, and a charge of +1.00 (default probe atom in Sybyl) to calculate various steric and electrostatic fields. The default energy cut off for steric and electrostatic fields was 30 kcal/mol.

Internal Validation and Partial Least Squares (PLS) Analysis

Partial Least Square regression analysis was done on the training set to develop the correlation between the QSAR (CoMFA) models and biological activity[4]. The reliability of the developed models were evaluated through leave-one-out (LOO) internal validation method, which calculates the square of the cross-validation coefficient (q^2) and the optimal number of components (ONC). Other parameters for the evaluation of the model are the non-cross-validation coefficient (r^2) and standard error of estimate (SEE).

External Validation of the QSAR model

The predictive ability of developed CoMFA models were evaluated using the test set. The predictive factor $r^2(r^2_{pred})$[5] was calculated using the predicted activity of the test set as follows:

$$r^2_{pred} = \frac{SD - PRESS}{SD}$$

where, SD= sum of squared deviation between the biological activity of molecules in the test set and mean biological activity of the training set molecules; PRESS= the sum of squared deviations between actual and predicted activity values for each molecule in the test set

RESULTS AND DISCUSSION

The 3D-QSAR models were obtained using a training set of 34 compounds and a test set of 8 compounds. The statistical parameters related to CoMFA models can be found in Table 2. The best CoMFA models were generated employing a partial least square (PLS) analysis, which produced squared regression coefficient (r^2) and cross-validation coefficient (q^2). When squared regression coefficient (r^2) and cross-validation coefficient (q^2) > 0.5, the model is considered as significant one. As shown in Table 2, the best CoMFA model for antifungal activity showed q^2 of 0.578, r^2 of 0.923 and a very low standard error of 0.0177.

Table 2: Statistical parameters of the CoMFA models of antifungal and antibacterial activity

Sl. No.	Activity	ONC	q^2	r^2	r^2_{pred}	SEE	Steric bulk desirable (%)	Steric bulk undesirable (%)	Positive charge desirable (%)	Negative charge desirable (%)
1	Antifungal	3	0.578	0.923	0.94	0.0177	36.43	27.61	4.71	11.22
2	Antibacterial	4	0.127	0.878	*	0.0329	30.27	18.44	17.57	13.69

***as the q^2 of the antibacterial model is insignificant, r^2_{pred} was not calculated.**

The distribution of actual and predicted pMIC for training and test set are shown in Figure 2. This showed a good fit diagonally. Thus the model is highly significant and can be used for further study. But in case of antibacterial activity the CoMFA model showed statistically insignificant results, having a q^2 of -0.127. The actual and predicted antifungal and antibacterial activities (pMIC) and their respective residuals are shown in Table 3.

Table 3: Actual and predicted Antifungal and Antibacterial (pMIC) activity and their respective residuals.

Sl. No.	Codes	Antifungal activities			Antibacterial activities		
		Actual pMIC	Pred-pMIC	Residuals	Actual pMIC	Pred-pMIC	Residuals
1	4a	-1.2268	-1.2198	0.0070	-0.9253	-0.932	0.0067
2	4b	-1.2533	-1.2487	0.0046	-0.85	-0.8577	0.0077
3	4c	-1.1510	-1.179	0.0280	-0.8102	-0.8388	0.0286
4	4d	-1.1852	-1.1823	0.0029	-0.8970	-0.897	0.0000
5	4e	-1.1964	-1.1842	0.0122	-0.8721	-0.8919	0.0198
6	4f*	-1.1649	-1.1487	0.0162	-0.9965	-0.9599	0.0366
7	4g#	-1.1775	-1.201	0.0235	-1.0132	-0.8787	0.1345
8	4h#	-1.2345	-1.2364	0.0019	-0.7937	-0.814	0.0203
9	4i	-1.2309	-1.2486	0.0177	-0.7371	-0.7305	0.0066
10	4j	-1.2161	-1.205	0.0111	-0.8394	-0.8191	0.0203
11	4k*#	-1.1417	-1.1511	0.0094	-0.8273	-0.918	0.0907
12	4l	-1.1486	-1.1328	0.0158	-1.0207	-1.0116	0.0091
13	4m	-1.2005	-1.1933	0.0072	-0.9025	-0.9049	0.0024
14	4n	-1.2208	-1.1866	0.0342	-0.7092	-0.7143	0.0051
15	4o	-1.1498	-1.1516	0.0018	-1.0094	-0.9667	0.0427
16	4p	-1.1467	-1.1484	0.0017	-0.9595	-0.9682	0.0087
17	4q	-1.1367	-1.1637	0.0270	-0.9143	-0.9153	0.001
18	4r*#	-1.2206	-1.1815	0.0391	-0.8998	-0.917	0.0172
19	VJ19	-1.0538	-1.0744	0.0206	-0.9201	-0.852	0.0681
20	VJ20	-1.0944	-1.089	0.0054	-0.6674	-0.6964	0.029
21	VJ21	-1.0958	-1.1023	0.0065	-0.7371	-0.7364	0.0007
22	VJ22*	-1.0748	-1.0848	0.0100	-0.8102	-0.8221	0.0119
23	VJ23	-1.0962	-1.0775	0.0187	-0.8830	-0.8824	0.0024
24	VJ24#	-1.0704	-1.0831	0.0127	-0.8825	-0.8945	0.0120
25	VJ25	-1.0941	-1.0969	0.0028	-0.8082	-0.8547	0.0465
26	VJ26	-1.1031	-1.1255	0.0224	-0.8739	-0.8169	0.0570
27	VJ27	-1.1251	-1.1175	0.0076	-0.9143	-0.9574	0.0431
28	VJ28*	-1.0941	-1.0967	0.0026	-0.8842	-0.856	0.0282
29	VJ29	-1.0704	-1.0833	0.0129	-0.8853	-0.8875	0.0022
30	VJ30	-1.0906	-1.1055	0.0149	-1.0128	-1.0067	0.0061
31	VJ31#	-1.0755	-1.0697	0.0058	-0.8692	-0.9209	0.0517
32	VJ32#	-1.0877	-1.0668	0.0209	-0.9201	-0.7625	0.1576
33	VJ33	-1.0941	-1.0601	0.0340	-0.9740	-0.9157	0.0583

34	VJ34	-1.0599	-1.0672	0.0073	-0.9278	-0.9434	0.0156
35	VJ35	-1.0228	-1.0419	0.0191	-0.85	-0.9399	0.0899
36	VJ36*	-1.0390	-1.1501	0.1111	-1.0314	-1.0349	0.0035
37	VJ37	-1.1280	-1.1394	0.0114	-0.8739	-0.8869	0.0130
38	VJ38*	-1.0962	-1.187	0.0908	-0.8061	-0.8078	0.0017
39	VJ39	-1.1731	-1.1508	0.0223	-0.8549	-0.8524	0.0025
40	VJ40*#	-1.1835	-1.1538	0.0297	-0.9642	-0.8391	0.1251
41	VJ41	-1.1950	-1.1698	0.0252	-0.9278	-0.9343	0.0065
42	VJ42	-1.1708	-1.1695	0.0013	-0.8715	-0.8832	0.0117

***test set molecule in antifungal CoMFA model; #test set molecule in antibacterial CoMFA model.**

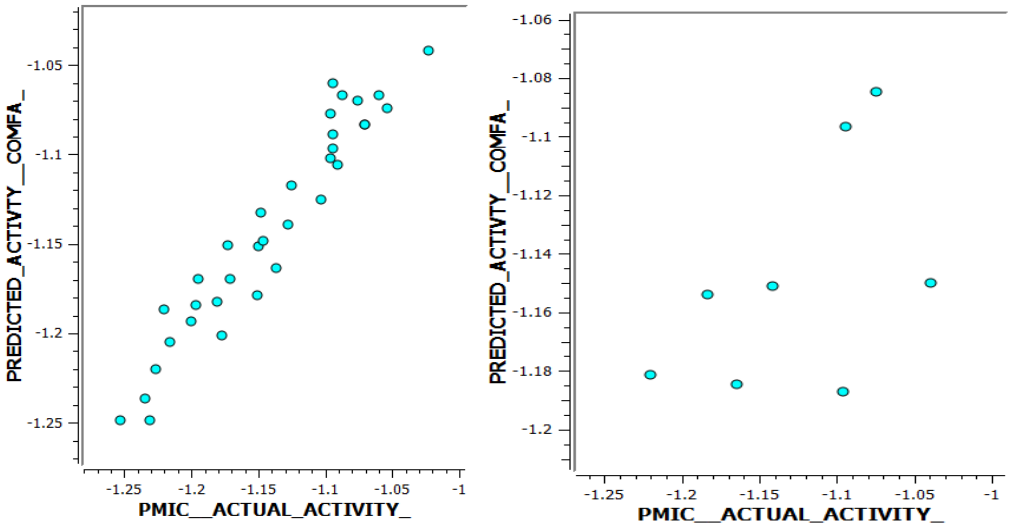

(A) (B)

Figure 2: Plots of Actual versus Predicted antifungal pMIC values for (A) training (B) test set.

During calculation of predictive factor r^2(r^2_{pred}), predicted pMIC of two compounds in the test set (code- VJ 36 and VJ 38) were excluded. It is clear from the Figure 2(B) that these two compounds are not in the diagonal line and behaving as outliers. The r^2_{pred} for antifungal CoMFA model is 0.94 (>0.5) which is highly significant, indicating good predictive ability of the model.

The CoMFA contour maps of most potent compound for antifungal activity and for antibacterial activity are shown in Figure 3 and Figure 4 respectively. The electrostatic contour map (Figure 3A for antifungal activity and Figure 4A for antibacterial activity) has blue and red regions. The blue regions indicate that presence of an electropositive group near them may increase the activity. While the red areas favors an electronegative group for better activity. In the other hand the steric contour map (Figure 3B and Figure 4B, for antifungal and antibacterial activity respectively) comprises of green and yellow regions. The green areas indicate that bulky groups (such as benzene ring) near them increase activity. While in the green areas presence of bulky groups decrease the activity.

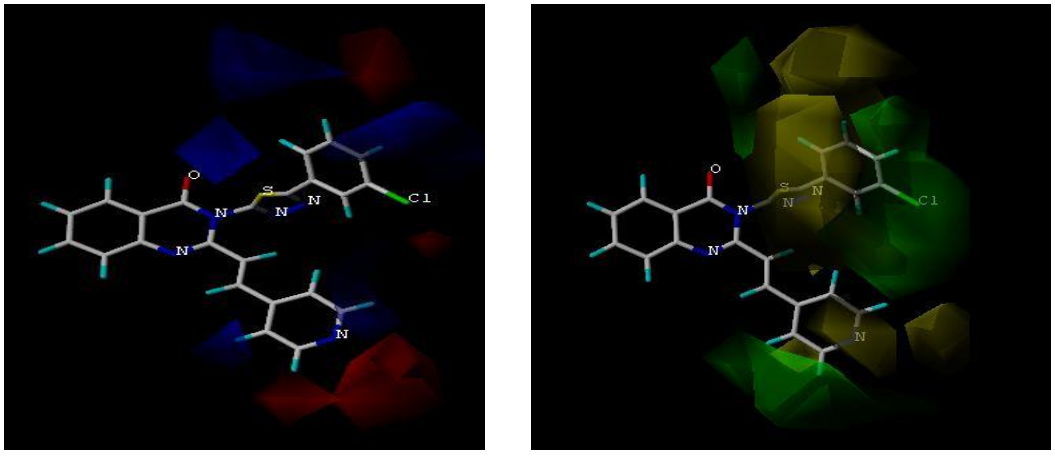

(A) **(B)**

Figure 3: CoMFA contour maps for antifungal activity displayed with most potent compound, VJ35. (A) CoMFA electrostatic contour map (blue, electropositive favored; red, electronegative favored); (B) CoMFA steric contour map (green, favored; yellow, disfavored).

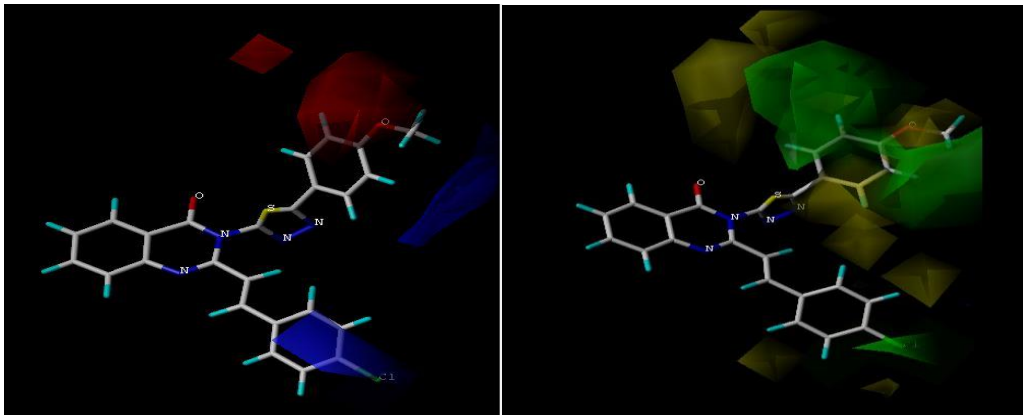

(A) (B)

Figure 4: CoMFA contour maps for antibacterial activity displayed with most potent compound, VJ20. (A) CoMFA electrostatic contour map; (B) CoMFA steric contour map.

Design of Compounds

Based on the CoMFA model obtained along with the help of contour maps for the antifungal activity several new molecules are designed. The chemical structures of the newly designed compounds and their predicted pMIC values are presented in Table 4.

The contour maps of the top ranked newly designed eight compounds 7, 19 & 4; 15, 14 & 16; 18 & 11, are presented in Figure 5, Figure 6 and Figure 7 respectively. The 3D QSAR studies reported here, could be used in the further modification and optimization of 4(3H)-quinazolinone derivatives for improved microbial activities.

Table 4: Designed compounds using CoMFA and their predicted antifungal activity.

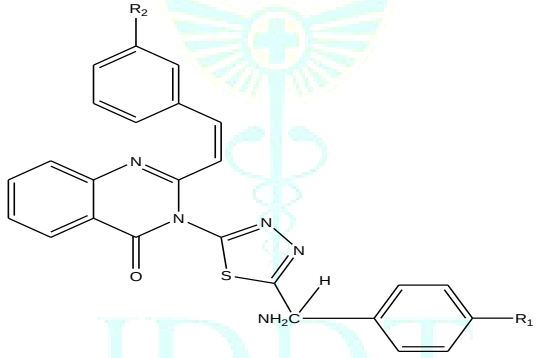

Compound No.	R_1	R_2	Predicted pMIC
1	-Cl	-H	-1.1258
2	-Br	-H	-1.1172
3	$-NO_2$	-H	-1.1208
4	-Cl	-Cl	-1.0805
5	-Br	-Cl	-1.1493
6	-F	-Cl	-1.1324
7	$-NO_2$	-Cl	-1.0372
8	$-CH_3$	-Cl	-1.1193
9	$-C_2H_5$	-Cl	-1.1256
10	$-OCH_3$	-Cl	-1.1311
11	$-OC_2H_5$	-Cl	-1.1108
12	-Cl	$-NO_2$	-1.163
13	-Br	$-NO_2$	-1.1233
14	-F	$-NO_2$	-1.0921
15	$-NO_2$	NO_2	-1.0891
16	-Cl	$-CH_3$	-1.0946
17	-Br	$-CH_3$	-1.1287
18	-Cl	$-OCH_3$	-1.1003
19	-Br	$-OCH_3$	-1.0706
20	-F	$-OCH_3$	-1.1458
21	$-NO_2$	$-OCH_3$	-1.1577

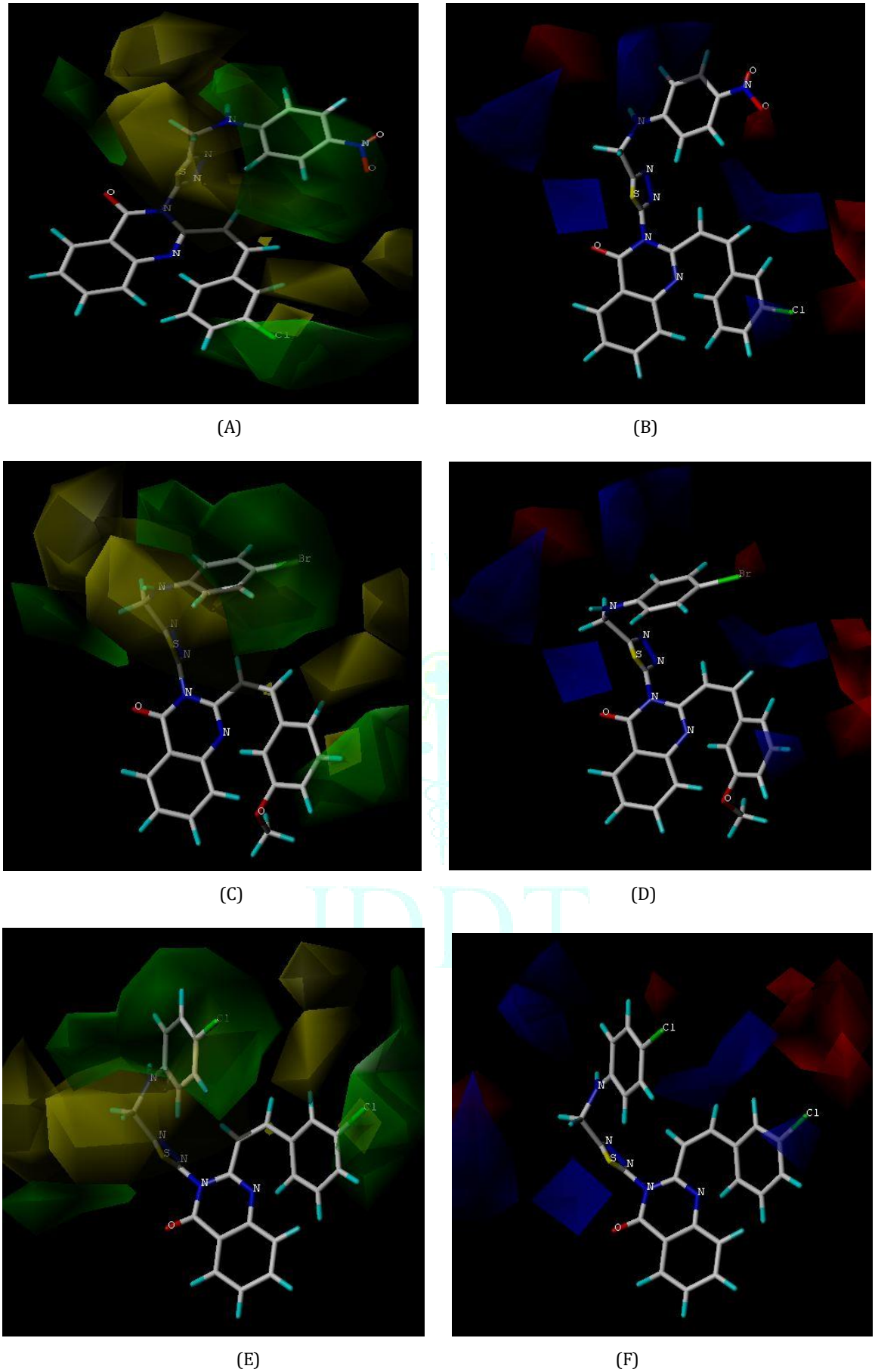

Figure 5: CoMFA contour maps with top ranked predicted antifungal activity of designed compounds (A) Steric, (B) Electrostatic, contour map of compound 7; (C) Steric, (D) Electrostatic, contour map of compound 19; (E) Steric, (F) Electrostatic, contour map of compound 4.

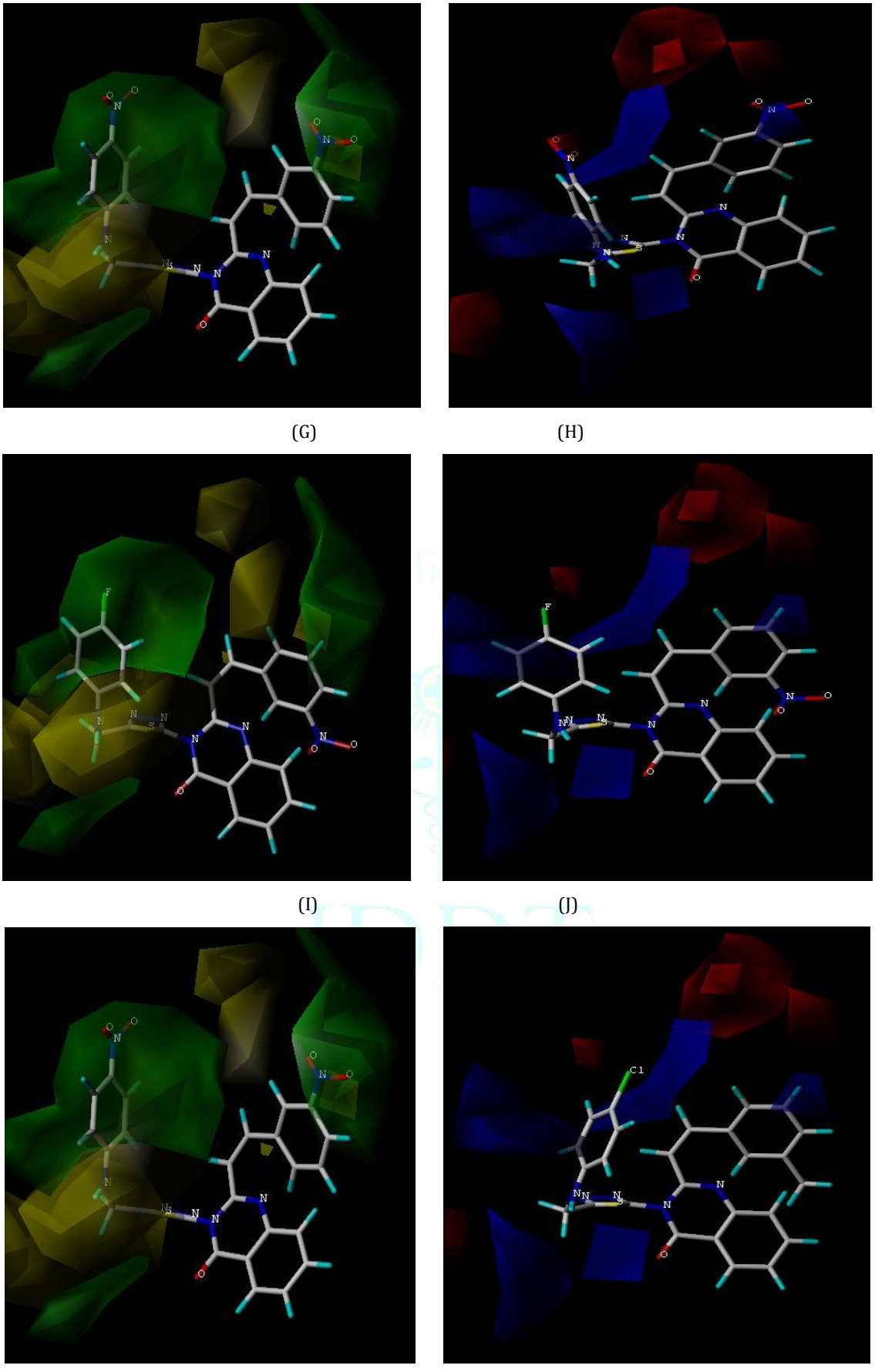

Figure 6: CoMFA contour maps with predicted antifungal activity of designed compound 15, 14, 16. (G) Steric, (H) Electrostatic, contour map of compound 15; (I) Steric, (J) Electrostatic, contour map of compound 14; (K) Steric, (L) Electrostatic, contour map of compound 16.

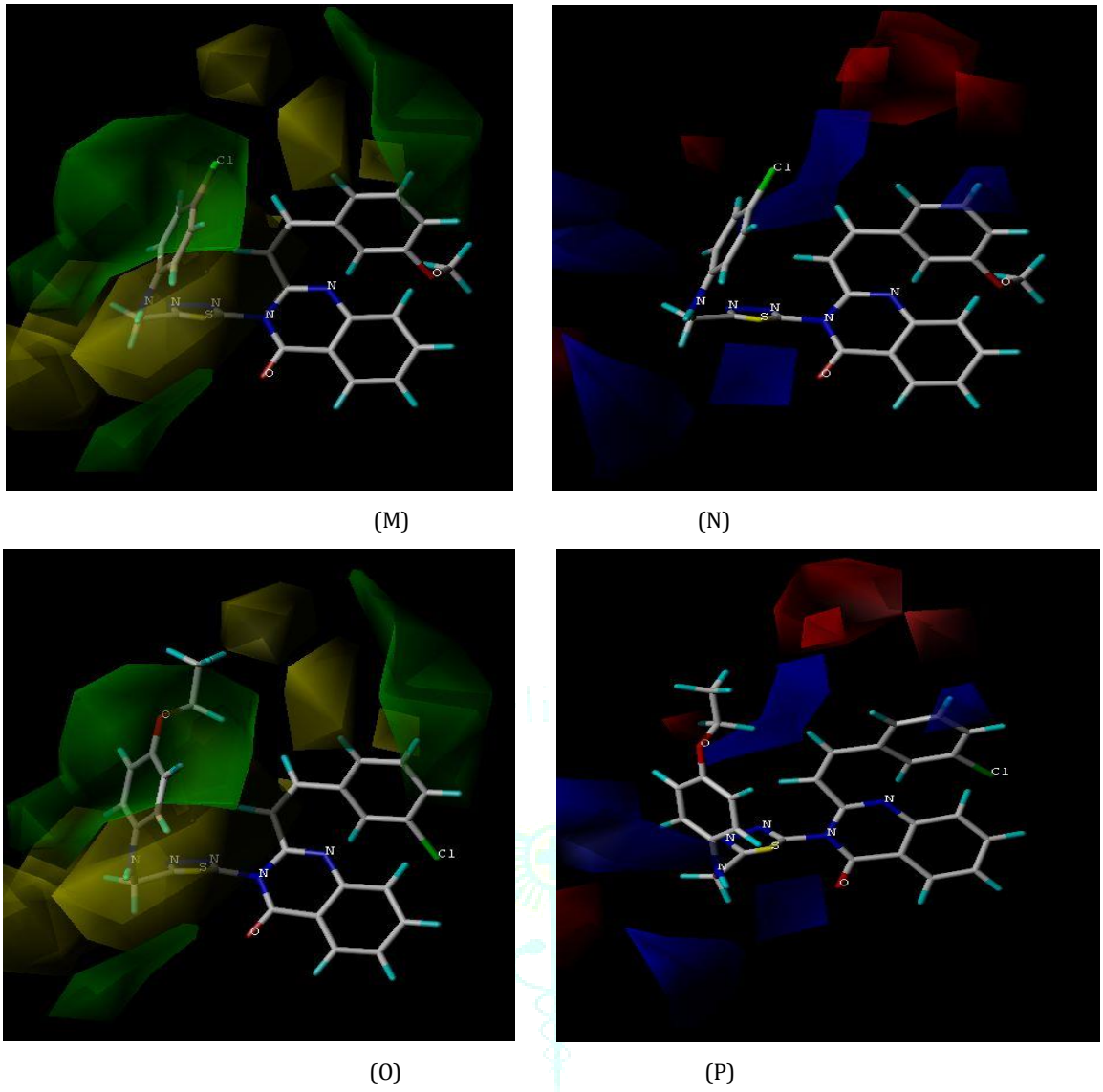

(M) (N)

(O) (P)

Figure 7: CoMFA contour maps with predicted antifungal activity of designed compound 18, 11. (M) Steric, (N) Electrostatic, contour map of compound 18; (O) Steric, (P) Electrostatic, contour map of compound 11.

CONCLUSIONS

3D QSAR based CoMFA were performed on reported series of 4(3H)-quinazolinone derivatives to investigate the spatial structural requirements to develop potent and significant antimicrobial compounds. The developed CoMFA model for antifungal activity was statistically very significant and used to design novel compounds. Out of many hypothetical compounds designed twenty one compounds were selected based on their predicted activity. Based on the information derived from the contour maps several new compounds were designed and their activities were predicted. The authors are planning to synthesize these screened compounds.

ACKNOWLEDGEMENT

Mr. Sumit Bhattacharya wish to thanks Chancellor and Vice Chancellor, Swami Vivekanand University, Sagar, Madhya Pradesh, India for their help throughout the research activity.

REFERENCES

1. Jatav V, Kashaw S, Mishra P, Synthesis, antibacterial and antifungal activity of some novel 3-[5-(4-substituted phenyl) 1,3,4-thiadiazole-2-yl]-2-styryl quinazoline-4 (3H)-ones. Medicinal Chemistry Research 2008; 17(2-7):169-81.
2. Dixit A, Kashaw SK, Gaur S, Saxena AK, Development of CoMFA, advance CoMFA and CoMSIA models in pyrroloquinazolinesas thrombin receptor antagonist, Bioorganic & Medicinal Chemistry 2004; 12(13):3591-8.
3. Jian Y, He Y, Yang J, Han W, Zhai X, Zhao Y, Li Y, Molecular modeling study for the design of novel peroxisome proliferator-activated receptor gamma agonists using 3D-QSAR and molecular docking. International Journal of Molecular Sciences 2018; 19(2):630-35.
4. Clark M, Cramer III RD, Van Opdenbosch N, Validation of the general purpose Tripos 5.2 force field. Journal of Computational Chemistry 1989; 10(8): 982-1012.
5. Golbraikh A, Tropsha A, Beware of q2, Journal of molecular graphics and modelling, 2002; 20(4):269-76.